Research Paper

Bioavailability Effect of Methylprednisolone by Polymeric Micelles

Ching-Lin Chen,[1] Shwu-Fen Chang,[2] Daniel Lee,[3] Lang-Yo Yang,[4] Yi-Hsuan Lee,[4] Chung Y. Hsu,[5] Shwu-Jiuan Lin,[3] and Jiahorng Liaw[3,6]

Purpose. To investigate the effect of PEO-PPO-PEO polymeric micelles (PM) formulation on the bioavailability of methylprednisolone (MP), a treatment of spinal cord injury (SCI), to the blood and spinal cord (SC) of rabbits.

Methods. The characteristic of MP formulated with PM (MP/PM) was evaluated by critical micelles concentration (CMC), dynamic light scattering (DLS), atomic force microscopy (AFM) and *in vitro* kinetic release measurements. HPLC was used to analyze the MP disposition in plasma and SC of rabbits receiving single dose intravenous administration. After MP/PM delivery, the mRNA and protein levels of anti-apoptotic marker, Bcl-x$_L$, were monitored by Reverse Transcription -Real-Time -Polymerase Chain Reaction (RT-qPCR) and Western blotting analysis, respectively.

Results. At a concentration of 0.1% and at 25°C, PEO-PPO-PEO copolymers formed micelles shown by fluorescence probe, DLS and solubility test. The size of the MP/PM was in an average of 60 nm with a single, rounded shape detected under AFM. Being formulated with 6% PM, MP had higher solubility (219.6 ± 3.6 μg/ml) and release rate (11.1 ± 0.4 ng min$^{1/2}$) at 37°C. After intravenously administrated with single dose of 1 mg/kg of MP/PM to rabbits, higher levels of MP in plasma and SC were detected compared to animals receiving an equal dose of MP, analyzed by HPLC. PM formulation markedly increased (7-fold) the plasma half-lives ($t_{1/2}$) of MP (from 76.1 ± 8.0 to 514.3 ± 70.0 min). In addition, the SC $t_{1/2}$ of MP/PM also increased from 278 to 528 min. In SC, the mRNA level of Bcl-x$_L$ increased 4-fold in animals receiving MP/PM compared to that with MP alone at 7 h post-administration. Similar elevated Bcl-x$_L$ protein was also detected upon MP/PM administration compared to MP.

Conclusions. PM vehicle was able to deliver MP to improve its pharmacokinetic profile in plasma and SC with higher expression of anti-apoptotic Bcl-x$_L$ at both mRNA and protein levels.

KEY WORDS: Bcl-x$_L$; bioavailability; methylprednisolone; PM; spinal cord.

INTRODUCTION

High-dose methylprednisolone (MP) has been shown to be an effective treatment and reduce apoptosis following spinal cord injury (SCI), in a glucocorticoid receptor (GR)-dependent manner (1–3). Furthermore, a decrease in the anti-apoptotic proteins (TNF-alpha, NF-kB, and Bcl-x$_L$ *et al.*) detected after

SCI was abrogated by MP treatment (3–7). The Third National Acute SCI Study demonstrated that patients receiving an intensive 24- to 48-h multiple intravenous MP regimen (30-mg/kg bolus dose plus 5.4 mg/kg/h) within 8 h of the injury had improved 6-month recovery compared with placebo-treated patients (1). However, this "megadose" steroid therapy was accompanied with adverse effects. Patients in the MP treatment groups experienced a 2.6-fold increase in the incidence of severe pneumonia and sepsis, an increased incidence of wound infection, an increased number of days spent receiving mechanical ventilation, and an increased number of days spent in the intensive care unit (1,8). These complications are believed to result from GR-induced immune suppression (9,10). In addition to these documented complications, there are also valid theoretical concerns associated with high dose glucocorticoid therapy in the setting of neural injury. These include steroid-induced hyperglycemia and sepsis-related hypotension, both of which may contribute to secondary neuronal injury (11–13). This may explain why some studies with high-dose steroids for SCI have failed to demonstrate therapeutic benefit.

Furthermore, the needs of megadose MP were also correlated to low bioavailability of MP in spinal cord area and to short elimination half-lives for insufficient effect-duration time

[1] Neurosurgical Department, Shin Kong Wu Ho-Su Memorial Hospital, No.95, Wen Chang Road, Shih Lin District, Taipei Taiwan.

[2] Graduate Institute of Cell and Molecular Biology, Graduate Institute of Medical Science, School of Medicine, Taipei Medical University, 250 Wu Hsing St., Taipei 110, Taiwan.

[3] College of Pharmacy, Taipei Medical University, 250 Wu Hsing St., Taipei 110, Taiwan.

[4] Department of Physiology, School of Medicine, Taipei Medical University, 250 Wu Hsing St., Taipei 110, Taiwan.

[5] Department of Internal Medicine, School of Medicine, Taipei Medical University, 250 Wu Hsing St., Taipei 110, Taiwan.

[6] To whom correspondence should be addressed. (e-mail: jhorng@tmu.edu.tw)

profile (11). In addition, recent reports have indicated that P-glycoprotein (MDR1)-mediated exclusion of MP from the spinal cord (14,15) and that MDR1 is capable of interfering with the absorption of MP in the rat small intestine (16). Poor response to the MP therapy was therefore, proposed to be possibly due to incomplete absorption of the MP by over-expression of MDR1 in the GI tract. On the other hand, the blood-brain barrier (BBB) and reticuloendothelial system (RES) limit the potential intravenous administration to achieve appreciable penetration to the brain and spinal cord (17,18). Therefore, the nervous system presents unique challenges for vector-based MP delivery. A need exists for the development of carrier-delivery to the nervous system such as, low immnuosupression, stable in the physiological environments, long circulation time and deliverable target size/methods. Among different carriers used for controlled drug delivery, many studies have focused on synthesized polymeric micelles which may have better solubility as well as the potential for large-scale production (19–24). Among non-ionic polymeric micellar carriers, the non-ionic PEO-PPO-PEO triblock copolymer micelles (PM) has been approved non-immunogenic, resistant to protein absorption, capable of inhibiting P-glycoprotein activity and stable in blood stream in the medical, pharmaceutical, and cosmetic fields (20,25,26). This copolymer with hydrophilic corona of PEO chain and hydrophobic PPO polymer core, can self-assemble to form nano polymeric micelles and encapsulate molecules with poor water solubility (20,26). Reports have indicated that PM with PEO chain can inhibit P-glycoprotein activity and protein absorption, therefore, it becomes a stable carrier with a sustained release in blood circulation (23–28).

The nano-sized (<150 nm) character of polymeric micelles prevents their uptake by the RES and facilitates their extravasations at leaky sites of capillaries, leading to passive accumulation in certain tissues and organs (28). The small nano size of these PM may also ease further penetration of micellar carrier through BBB into the CNS system (20,29), and increase the transport of drug across membrane of BBB by membrane perturbance (20,26). The lower toxicity and non-immunogenic properties of PM carrier have been also proved by the Food and Drug administration (30). Other advantages related to the nanoscopic dimensions of this PM include the ease of sterilization via filtration and safety of administration. Therefore, a multifunctional nature of this nano PM appears to fulfill several tasks required for an ideal carrier capable of selective drug delivery.

The main purpose of this study is to evaluate the pharmacokinetic profiles of MP in the systemic blood and local spinal cord levels delivered with PM formulation. In addition, anti-apoptotic Bcl-x_L protein level was also investigated by MP/PM treatment in SCI model.

EXPERIMENTAL

Animals

Male New Zealand rabbits (National Laboratory Animal Center, Taipei, Taiwan) weighing approximately 1.5~2.0 kg were used for all *in vivo* pharmacokinetic studies. Six to eight weeks-old male nude mice (BALB/cAnN.Cg-*Foxn1nu*/CrlNarl) were used for *in vivo* intravenous delivery studies in SCI model and were purchased from the National Laboratory Animal Center (Taipei, Taiwan). The protocols were approved by the Laboratory Animal Research Committee of Taipei Medical University, and were maintained under specific pathogen-free conditions. Animals were fasted for 48 h before the experiment with free access to water.

Materials

MP was purchased from Sigma Co. (St. Louis, MO, USA). Poly(ethylene oxide)-poly(propylene oxide)-poly(ethylene oxide) (PEO-PPO-PEO) copolymer, with an average molecular mass of 8,400 Da, was obtained from BASF (Ludwigshafen, Germany). Acetonitrile (HPLC grade) was obtained from BDH Laboratory Supplies (Pools, UK). All chemicals were of reagent or analytical grade and were used as received.

Determination of the Critical Micelle Concentration (CMC) of PEO-PPO-PEO Polymeric Micelles (PM)

The formation of PEO-PPO-PEO PM was confirmed by a fluorescence probe technique using pyrene; the partition of pyrene into the micellar phase was determined using the ratio of peak I_1/peak I_3 of the pyrene spectrum as previously reported (25,31,32). The fluorescence emission spectra of pyrene in the PEO-PPO-PEO polymeric micelles solutions were measured from 350 to 500 nm using a fixed excitation wavelength of 339 nm with a constant pyrene concentration of 6×10^{-7} M. The concentration of PEO-PPO-PEO polymers used varied from 1×10^{-4} to 10% (w/w). Spectral data were acquired using a Hitachi F-4500 fluorescence spectrophotometer (Hitachi, Tokyo, Japan). All fluorescence experiments were carried out at 25°C.

Preparation of Methylprednisolone/PEO-PPO-PEO PM (MP/PM)

An excess amount of MP was added to 0.0001–10% (w/v) PM and mixed by vortexing. The mixture was then kept at 25°C for 3 days to get to equilibrium. The equilibrated sample was centrifuged at 1,000 rpm for 10 min to remove the undissolved MP. The supernatant was collected and diluted with methanol for quantification of MP by HPLC analysis. The MP alone was also added to 1 ml of water with stirring at 25°C for 3 days to get to equilibrium. The amounts of MP were quantified using a HPLC-UV system consisting of a pump, an auto-injector (LC-10AD and SIL-10AD Shimadzu (Kyoto, Japan), and a UV detector (SPD-10A vp, Shimadzu, Kyoto, Japan) with an integrator (EZ chrom™ Chromatography Data System Version 6, San Roman, CA, USA). Samples were injected into a Cosmosil 5C18-MS reverse-phase column, (250 × 4.6 mm, 5 μm, Merck); water/acetonitrile (66:34, pH 3.4) was used as the mobile phase. The flow was 1 ml/min with the detector set at 243 nm, and cortisone (20 μg/ml) was added to the sample solution as the internal standard. Calibration curves were obtained by plotting the peak height of the authentic drug as a function of drug concentration. The inter- and intra-day coefficients of variation of each assay were all less than 10%. The lower limit of quantitation of MP was 5 ng/ml. In addition, MP was tested in PBS solution and no significantly degradation of MP was observed at 37°C for 12 h.

Size and Zeta Potential of MP/PM

The size and Zeta potential of formulation containing MP and 6% PM solution were measured and compared with mixtures containing either MP alone or 6% PM solution alone. The average particle size and Zeta potential of MP/PM were determined by quasielastic laser dynamic light scattering (DLS) (Zetasizer 3000; Malvern Instruments, Malvern, UK), using an assumed refractive index ratio of 1.33 and a viscosity of 0.88 (31,32). The sampling time for each sample was 10 μs and the experimental duration was 100 s. All measurements were performed at 25°C at a measurement angle of 90° and results were presented as mean ± S.E.M.

Atomic Force Microscopy (AFM)

Ten microliters of MP/PM were placed on a mica surface with no further treatment. The AFM (CP-II; Digital Instruments/Veeco Metrology Group, Santa Barbara, CA) was operated in constant tapping mode, as described in the previous study (31). The cantilevers were standard NanoProbe silicon single-rectangular cantilevers (NSC15/AIBS 230 μm) (Mikro-Masch, Estonia); the constant force mode was used with a typical scan frequency of 328 kHz. A scanner with 1-μm scanning range was used, and all images were collected within $3 \times 3 \ \mu m^2$ area. Unless otherwise stated, all images shown were subjected only to the normal image processing of leveling.

In Vitro Membrane Release of MP

In order to study the effect of PM on MP release, a Franz cell with a cellulose membrane (active diffusion area 0.627 cm^2) was used for the *in vitro* release studies (25). MP or MP/PM formulation (500 ng in 0.5 ml) was placed to the donor compartment and 6 ml of pH 7.4 phosphate buffer solution (PBS) in the receiver compartment. The diffusion cells were maintained at 37°C in a water bath (SR70, Shimaden, Tokyo, Japan), and stirring was set at 700 rpm throughout experiment. Samples (0.6 ml) were withdrawn from the receiver compartments at fixed intervals and replaced with an equal volume of pre-warmed PBS. The MP samples were assayed by the HPLC-UV method. The release time profile of MP was obtained by plotting cumulative amount of MP released against time.

In Vivo Pharmacokinetic Study

Male New Zealand rabbits were fasted for 12 h before each experiment but allowed free access to water. MP was dissolved with 6% PM (MP/PM) for intravenous dosing. Rabbits were given with MP/PM or MP solution intravenously at doses of 1 mg/kg within 3 min administration. At predetermined intervals, blood samples (1 ml) were collected from an ear vein and centrifuged at 3,000 rpm for 10 min, and stored at −20°C before HPLC analysis. Spinal cords were collected from rabbits after 5% pentobarbital injection through vein and then were stored at −20°C before HPLC analysis.

Methylprednisolone (MP) Assay in Plasma and Spinal Cord

The MP plasma samples were determined chromatographically by an HPLC-UV system consisting of a pump, an auto-injector (LC-10AD and SIL-10AD Shimadzu (Kyoto, Japan), and a UV detector (SPD-10A vp, Shimadzu, Kyoto, Japan) with an integrator (EZ chrom™ Chromatography Data System Version 6, San Roman, CA, USA). Plasma (0.5 ml) and 10 μl of dexamethasone (20 μg/ml), as the internal standard, were denatured with methanol (0.6 ml) and centrifuged at 13,000 rpm for 5 min, and 100 μl of the supernatant was injected into a Cosmosil 5C18-MS reverse-phase column, (250 × 4.6 mm, 5 μm, Merck); water/acetonitrile (66:34, pH 3.4) was used as the mobile phase. The MP in spinal cord sample (50 mg) and 10 μl cortisone (20 μg/ml), as an internal standard, were mixed with 100 μl water and denatured with methanol (0.6 ml) and centrifuged at 3,000 rpm for 15 min, and 100 μl of the supernatant was injected into a Biosil 5U ODS-U column (250 × 4.6 mm, 5 μm, Merck) with 0.01 M phosphate buffer / acetonitrile (84:31, pH 7.4). The flow was at 1 ml/min with the detector set at 243 nm. All calibration curves were obtained by plotting the peak height of the authentic drug as a function of drug concentration. The inter- and intra-day coefficients of variation of each assay were all less than 10%. The lower limit of quantitation of MP was 20 ng/ml and 10 ng/mg for plasma and spinal cord sample, respectively. The recovery of MP with the blank plasma and spinal cord were at least 82 and 72%, respectively.

Pharmacokinetic Data Analysis

Individual data of MP concentrations in plasma and spinal cord after intravenous administration were analyzed using noncompartmental analytic model (WinNonlin 4.1, Pharsight Corporation, Mountain View, CA, USA). Differences in the area under the plasma concentration-time curve (AUC), terminal half-lives ($t_{1/2}$) of plasma and spinal cord, clearance (Cl), terminal volume of distribution (Vss), and the mean residence time (MRT) between MP and MP/PM were compared by one-way ANOVA analysis followed by the post-hoc Scheffe test and the differences were considered to be significant at a level of $p < 0.05$. Because of the limit of detection of the assay (20 ng/ml for plasma, 10 ng/mg for spinal cord), the plasma and spinal cord concentration of MP could not be measured up to the last sampling time point at 9 and 10 h, respectively. $AUC_{0-\infty}$ was calculated, using Ct/β, with Ct being the last measured concentration. The elimination half-life ($t_{1/2}$) values were calculated from ln2/β, where β is calculated by log-linear regression analysis of the terminal log-linear phase. Total body clearance (Cl) was estimated by dividing the dose by area under the plasma concentration-time curve (AUC). Volume of distribution at steady state (Vss) was estimated based on statistical moment analysis. The mean residence time (MRT) of MP in the body for each dose was estimated by $MRT = AUMC_{0-\infty}/AUC_{0-\infty}$, where $AUMC_{0-\infty}$ is the area under the moment curve from zero to infinity.

Spinal Cord Injury (SCI)

Due to size limited of SCI impactor, SCI was induced in adult female mice (20 ± 5 g) with characterized New York University MASCIS impactor as our previously studies (33). Under halothane anesthesia (induction 4%, maintenance 2%, in an oxygen and nitrous oxide 50:50 mixture), a T9–T10

laminectomy was performed and the spinal cord was injured by dropping a 10-g weight from a height of 25 mm. Sham-operated controls were laminectomized, but were not contused. The incisions were closed and mice were returned to their cages after recovering from anesthesia. Mice surviving for 24 h after the injury underwent manual bladder expression. Injured mice were delivered with MP formulated of PM or MP alone after SCI. A segment of spinal cord (0.8 cm) covering the epicenter of injury was removed and used immediately for Western blotting and total RNA extraction.

Reverse Transcription -Real-Time -Polymerase Chain Reaction (RT-qPCR)

Total spinal cord RNA was extracted with TRIzol reagent (Invitrogen Life Technologies, Carlsbad, CA) according to the manufacturer's instructions. cDNA was prepared with Super-Script II reverse transcriptase (Invitrogen Life Technologies) as previous studies (32,33); quantitative real-time PCR was then performed on ABI PRISM 7300 sequence detection systems (Applied Biosystems, Foster city, CA, USA). The sequence of the primers used were as followings: mouse Bcl-x_L forward primer (on exon 2), 5′-AGG CTG GCG ATG AGT TTG AA-3′; mouse Bcl-x_L reverse primer, 5′-TGA AAC GCT CCT GGC CTT TC-3′ (34,35). Mouse GAPDH was chosen as the housekeeping gene for comparative analysis (forward primer, 5′-TGG TAT CGT GGA AGG ACT CAT GAC-3′, primer, 5′-ATG CCA GTG AGC TTC CCG TTC AGC-3′) (36). The qPCR amplifications were performed in 25 μl reaction mixtures containing 5 μl cDNA (1:4 diluted), 12.5 μl mastermix with SYBR® Green I containing a hot-start polymerase and a final concentration of 3 mM $MgCl_2$ (Applied Biosystems, Foster city, CA, USA), and 200 nM for GAPDH primers or 500 nM for Bcl-x_L primers. Thermocycling was carried out for 2 min at 50°C, 10 min at 95°C, and over 40 cycles of 15 s at 95°C, 1 min at 60°C. At the end of the PCR cycles, amplification specificity was confirmed by dissociation curve analysis and the products were separated on 3% agarose gel and stained with ethidium bromide for visual confirmation of PCR products. The quantification values were obtained from the threshold cycle (Ct) number at which the increase in signal associated with an exponential growth of PCR products began to be detected using SDS software. The fold change in Bcl-x_L expression relative to the GAPDH endogenous gene control was determined by: fold change = $2^{-\Delta(\Delta C_T)}$, where $\Delta C_T = C_{T(Bcl-xL)} - C_{T(GAPDH\,RNA)}$ and $\Delta(\Delta C_T) = \Delta C_{T(Bcl-xL/MP/PM\,or\,MP\,alone)} - \Delta C_{T(Bcl-xL)}$. C_T is the threshold cycle determined at 84 for fluorescence data collection. All results were presented as Mean ± S.E.M.

Western Blotting Analysis

Protein levels for Bcl-x_L in spinal cord tissue at 10 h after first dosing were detected by Western blotting analysis. Mice ($n = 5$ per group) were decapitated, and spinal cord fragments with 3 cm length centered at T10 were rapidly removed, weighed, and frozen at −80°C until use. Tissue homogenates were prepared by direct lysis with 2× SDS gel-loading buffer (100 mM Tris HCl pH 6.8; 200 mM dithiothreitol; 4% SDS; 0.2% bromophenol blue and 20% glycerol), lysates were mixed thoroughly and heated in boiling-water bath for 10 min, following by centrifugation (13,000 g for 10 min at 4°C). After collect the supernatant, protein concentrations were determined (37). Protein samples were separated on a SDS-polyacrylamide gel, and transferred overnight to methanol activated polyvinylidene difluoride (PVDF) membrane (Hybond-P; Amersham Biosciences, NJ, USA) at 4°C. Before incubating with antibody, the membranes were blocked for 1 h at room temperature in 5% nonfat dry milk in Tris-buffered saline (TBS). Primary antibody (a polyclonal rabbit anti-Bcl-x_L at 1:200 dilutions and a polycolonal rabbit anti-GAPDH at 1:300) was then added to the membrane and incubated overnight at 4°C. The membranes were then washed three times with 0.1% Tween 20 in TBS, incubated with horse-radish peroxidase (HRP)-conjugated goat anti-rabbit′ secondary antibody (1:500) for 1 h at room temperature. The immunoreactive complex was visualized by the ECL chemiluminescent substrate using the Amersham enhanced chemiluminescence's lighting system (ECL, RPN 2209; Arlington Heights, IL).

Statistical Analysis

All data are expressed as Mean ± S.E.M. Overall, inter-group comparisons were made using one-way ANOVA, and means of individual group were compared using the t statistic for least significant differences. Statistical significance of differences among means of groups was determined using Student's paired t test. Differences were considered to be significant at $p < 0.05$.

RESULTS

Characterization of Micelle Formation of PEO-PPO-PEO Copolymer with Methylprednisolone (MP)

By measuring the intensity ratios of the first to the third vibrational bands of pyrene at various concentrations of PEO-PPO-PEO copolymers in the presence of 6×10^{-7} M pyrene (with excitation at 339 nm) are shown in Fig. 1. The data showed that the I_1/I_3 peak height ratio decreased at copolymer concentration above 0.01% (w/w). The magnitude of I_1/I_3 (here 1.1) in solution with higher polymer concentration is similar to that of pyrene in toluene solution (1.04) and significantly lower than that in water (1.7). The ratio of
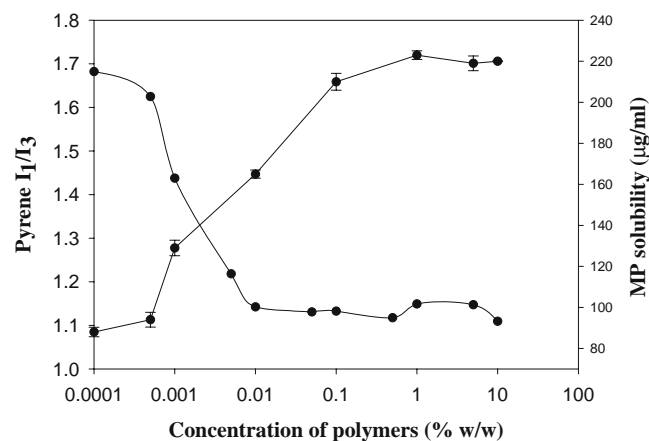

Fig. 1. The plot of intensity I_1/I_3 ratio of vibrational bands in the pyrene fluorescence spectrum and solubility of methylprednisolone (MP) as a function of PEO-PPO-PEO polymer concentration.

Table I. Characteristics of Methylprednisolone (MP) with PEO-PPO-PEO Polymeric Micelles (MP/PM)

	Particle Size (nm)	Zeta Potential (mV)	MP Solubility (μg/ml)
MP	–	−16.9 ± 5.4	70.8 ± 1.1
PM	62.7 ± 9.2	−3.8 ± 1.2*	–
MP/PM	47.4 ± 6.1	−6.2 ± 2.1*	219.6 ± 3.6*

Values are expressed as the mean ± S.E.M.
*Denotes a statistical significant increase ($p < 0.01$) compared to MP.

fluorescence intensities was usually correlated with the hydrophobicity of the molecular environment of the pyrene probe (19,21). In addition, the solubility of MP in PEO-PPO-PEO copolymers at various concentrations is shown in Fig. 1. The results showed that the solubility of MP increased with copolymer concentration until 0.1%. Taken together, these data indicated that at concentration above 0.1% of PEO-PPO-PEO copolymer, pyrene or MP should be relocated to the hydrophobic portion of the micelles. In the following study, polymer at 6% (w/w) concentration was used to form PM. By dynamic light scattering (DLS) particle size measurement, PEO-PPO-PEO copolymer at 6% (w/w) exhibited a single modular population distribution of particle within the 62.7 ± 9.2 nm range (Table I). MP/PM formulation of particle size by DLS measurement was observed around 47.4 ± 6.1 nm. The Zeta-potential of MP significantly increased from −16.9 ± 5.4 mV to −6.2 ± 2.1 mV after formulated with PM (Table I). In order to visualize the morphology of MP/PM, AFM was used. The shape of MP/PM was observed mainly being single, smooth and round (Fig. 2). The diameter of MP/PM formulation measured from one edge across the center to the other edge was 53–60 nm. It is notable that an increased solubility of MP in the presence of PM, in that the maximum MP solubility was 219.6 ± 3.6 μg/ml for MP/PM and 70.8 ± 1.1 μg/ml for MP alone (Table I).

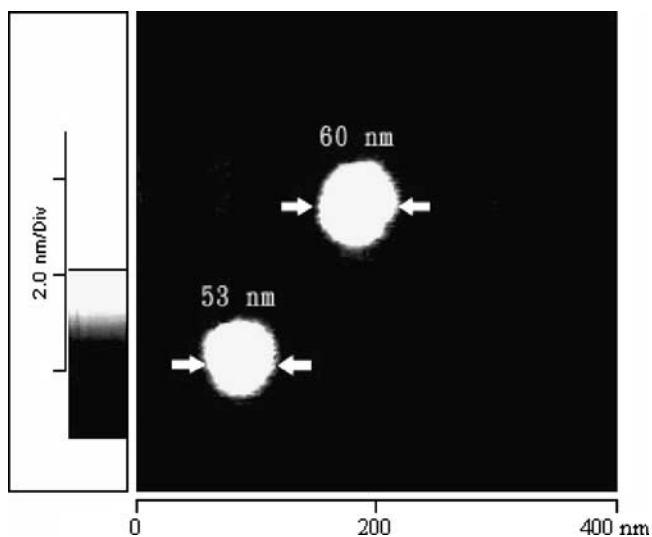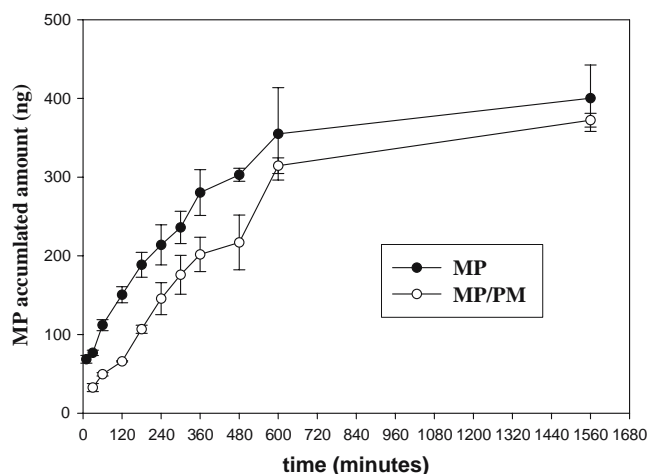**Fig. 3.** Effect of 6% PEO-PEO-PPO polymeric micelles (PM) on MP release from a cellulose membrane (each value represents the mean ± S.D. of $n = 3$).

Effect of PM on MP release

The release rates of MP from MP/PM formulation or in solutions were determined. Fig. 3 shows the cumulative amount of MP *versus* time in minutes. The release patterns indicate that PM with MP decreases the release rates of MP. In the presence of 6% copolymer, the rate of MP release was calculated by the least-squares Higuchi method ($Mr/M\infty = k\sqrt{t}$) (25) and to be 11.1 ± 0.4 ng min$^{1/2}$. However, the release rate of MP without PM was 9.3 ± 0.3 ng min$^{1/2}$.

In Vivo Intravenous Delivery of MP/PM

The bioavailability of MP/PM was evaluated and compared with MP solution as a control *in vivo*. The results are shown in Fig. 4 and indicate that MP was eliminated and
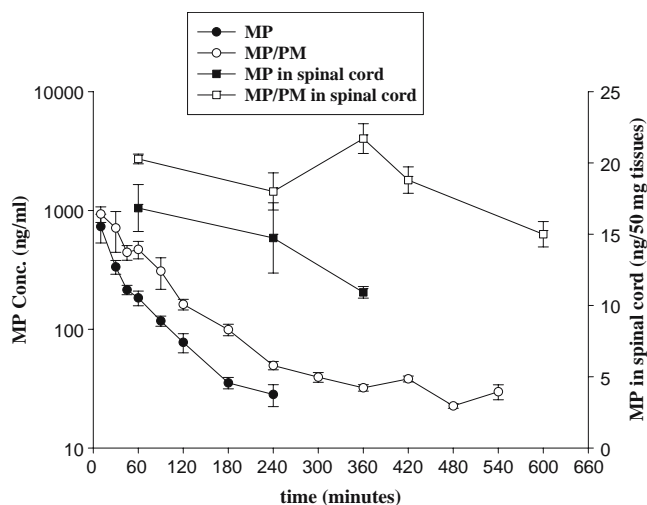

Fig. 2. AFM images of 10 μl of PEO-PEO-PPO polymeric micelles (PM) (6%) with MP on mica surface.

Fig. 4. Plasma and spinal cord concentrations–time curves of MP alone and MP with 6% PEO-PEO-PPO polymeric micelles (MP/PM) after intravenous administration of 1 mg/kg to six rabbits ($n = 6$) (each value represents the mean ± S.E.M.).

could not be detected at 4 h post-injection of MP only. However, relatively higher concentrations of MP were detected in plasma until 9 h after intravenous injection of MP/PM. The relevant pharmacokinetic parameters are listed in Table II. MP/PM formulation gave the higher AUC_{0-t} (89.8 ± 1.2 μg min/ml) compared to MP solution (39.9 ± 7.7 μg min/ml). Statistical analysis revealed that the AUC_{0-t} and $AUC_{0-\infty}$ of MP/PM were significantly higher ($p < 0.05$) than that of MP solution. The relative bioavailability of MP/PM increased by 2–3 folds compared to that of MP solution. The plasma half-live was significantly increased for MP/PM (514.3 ± 70.0 min) compared to that of MP (76.1 ± 8.0 min). MP with PM exhibited a smaller clearance (8.8 ± 1.5 ml/min) and longer mean residence time (MRT=463.6 ± 129.5 min). Although the spinal cord levels of MP alone were below the limit of quantitation after 360 min, substantial amounts of MP were still detected in the spinal cord with PM formulation until 600 min (Fig. 3) for dose of 1 mg/kg. The AUC_{0-t} of MP at spinal cord was also increased from 4,875 to 10,500 ng min for MP only and MP/PM administration, respectively (Table II); and the relative bioavailability of MP/PM increased by 2 folds compared to MP solution. The half-life of MP in spinal cords was increased from 278 to 528 min for MP only and MP/PM, respectively. MP with PM exhibited the smaller clearance (0.0001 ml/min) and longer mean residence time (MRT=303 min).

Anti-apoptotic Bcl-x_L Expression after Delivery of MP/PM

To further investigate the correlation between Bcl-x_L expression and MP delivered in the formulation with PM, we performed quantitative real-time PCR (qPCR) to determine the expression levels of Bcl-x_L in spinal cord tissues. A pair of primers specific to mouse GAPDH mRNA was included to serve as an internal control in the qPCR analysis. Our results indicated that the mRNA level of Bcl-x_L in spinal cord at 60 min after MP/PM and MP alone delivery were about 1.59 ± 0.21, 0.68 ± 0.12 folds compared that delivered with shamed-water

Table II. Non-compartment Pharmacokinetic Parameters of Intravenous Delivery of 1 mg/kg Methylprednisolone (MP) alone and MP with PEO-PEO-PPO Polymeric Micelles (MP/PM) in Rabbits ($n = 6$)

Parameters	MP	MP/PM
Plasma		
AUC_{0-t} (μg min/ml)	39.9 ± 7.7	89.8 ± 1.2*
$AUC_{0-\infty}$ (μg min/ml)	42.6 ± 7.9	140.0 ± 34.3*
$t_{1/2}$ (min)	76.1 ± 8.0	514.3 ± 70.0*
Vss (l)	2.8 ± 0.4	6.5 ± 1.3*
Cl (ml/min)	26.3 ± 3.0	8.8 ± 1.5*
MRT (min)	71.8 ± 6.1	463.6 ± 129.5*
Spinal cord (50 mg tissues)[a]		
AUC_{0-t} (ng min)	4,875	10,500
$t_{1/2}$ (min)	278	528
Cl (ml/min)	0.0002	0.0001
MRT (min)	181	303

Values are expressed as the mean ± S.E.M.

[a] Spinal cord (50 mg) was collected from each animal with one single time point and six animal experiments. Thus, values are expressed as the mean without S.E.M.

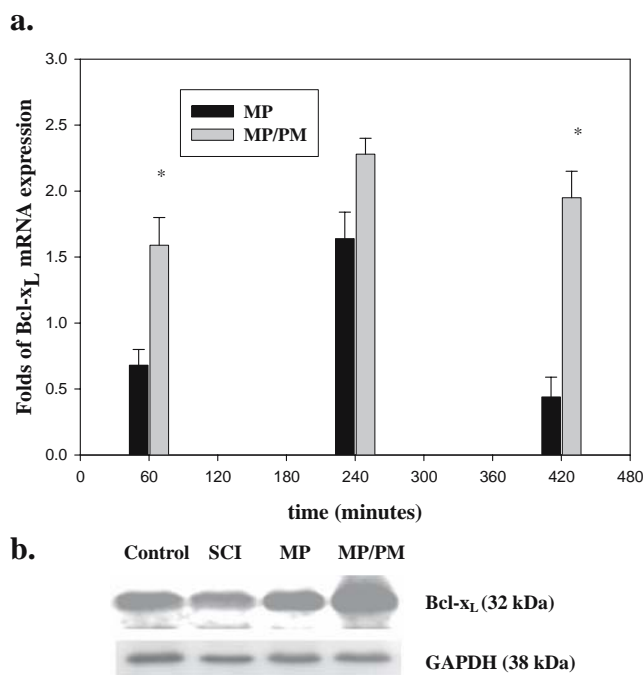*Denotes a statistical significant increase ($p < 0.01$) compared to MP alone.

Fig. 5. a Bcl-x_L expression correlated with MP delivery alone and with PEO-PPO-PEO polymeric micelles (MP/PM) on spinal cord injury (SCI) mice. MP delivery with PM (MP/PM) had higher expression level of Bcl-x_L as indicated by reverse transcription - real-time -PCR assay. *$p < 0.05$. A pair of primers specific to rabbits GAPDH mRNA was also included to provide an internal control. The graph represents the average of five independent assays using 2500 ng of total RNA, and the error bar indicated the S.E.M. **b** Representative Western blot for Bcl-x_L protein (33 kDa) 7 h after the first delivery of MP or MP/PM on spinal cord injury (SCI) mice. Shamed-watered control for loading was GAPDH.

control groups. Although at 240 min, in spinal cord levels of mRNA Bcl-x_L in spinal cord between MP with PM was expressed similar 1.64 ± 0.2 and 2.28 ± 0.12 folds, respectively (Fig. 5a), MP alone delivery were significantly decreased the expression of mRNA Bcl-x_L (0.44 ± 0.15) at 420 min. However, substantial the expression of mRNA Bcl-x_L (1.95 ± 0.20) with MP/PM were still observed at 420 min. There were no significant difference among shamed-water control groups and shamed-PM groups within 60, 240, 420 min (data no shown). In addition, Western blotting analysis with anti-Bcl-x_L antibody was used to confirm the gene expression at protein level after spinal cord injury (SCI) in mice. As shown in Fig. 5b, the level of Bcl-x_L protein with the expected size was increased upon MP treatment in the spinal cord of SCI mice, which was further elevated when MP delivery in the PM-formulated form.

DISCUSSION

In general, the half-live of free MP alone usually is short with a range of 1.5–2 h in rabbits, cat, rats and human being (38–40), and is similar to our results (71.8 ± 6.1 min). In addition, the Cl (13.1 ± 1.5 l/min/kg), Vss (1.4 ± 0.2 l/kg), and MRT (71.8 ± 6.1 min) of MP when delivered without PM were similar to the values reported in rabbits by Piekosewsk *et al.* (40), (15 ± 3 l/min/kg, 1.1 ± 0.25 l/kg and 144 ± 30 min, respectively). Other

investigators have shown that MP alone is rapidly concentrated in the spinal cord after a single i.v. bolus, with peak concentrations achieved by 10 min (38). Due to its greater lipid solubility, MP is expected to enter the central nervous system. Indeed, the MP content in spinal cord following i.v. administration was found to reach the steady state after 1 h (Fig 4). However, it has been shown that poor bioavailability of MP in spinal cord after i.v. administration is due to a p-glycoprotein-mediated exclusion of MP from the spinal cord (14). Indeed, our results showed that the MP in spinal cord declined after 1 h and could not be detected after 4 h.

Although MP is practically insoluble in aqueous media, several approaches, such as the preparation of prodrugs (dextran-MP) (41), and liposomal inclusion complexes (42) have been attempted to improve its water solubility. Their results show that the highly lipophilic MP molecules can be effectively incorporated into the delivery vehicles, providing a novel delivery system for MP with a prolonged release. Although the maximum amount of MP could be increased from 70 to 220 µg/ml, this PM only enhanced the solubility of MP by a factor of 3 compared with other PM such as poly(caprolactone)-b-poly(ethylene oxide) (PCL-b-PEO) could enhance 300 folds (29). However, the ideal vehicle-incorporated MP solution should not only provide the maximum content of MP, but also enhance the stability of MP in circulation and increase its transport across BBB membranes (27,37).

In addition, by coating with PEO or PEO-PPO-PEO, a number of studies have demonstrated the 'stealth' behavior of delivery that decreased the uptake or degradation by the reticuloendothelial system (RES) or reduced the adsorption by plasma proteins (43–46). Our $in\ vivo$ pharmacokinetic data (Fig. 4) indicated that the elimination half-life ($t_{1/2}$) of MP was 514.3 ± 70.0 min in the presence of PM and it is almost 7 times slower than MP only (76.1 ± 8.0 min). This was similar to other reports that the plasma circulation half-life of coated particles was increased from 20 to 780 min (43, 45). On the other hand, the nano size (<150 nm) of delivery carrier has been reported that it could ease further penetration of BBB into CNS system (20, 29). The major different pharmacokinetic profiles of MP with PM formulation in spinal cord were that MP would be detected after 240 min. We found that AUC, MRT, and half-life of MP formulated with PM in spinal cord were all higher than those of MP only. Thus, these suggest that PEO-PPO-PEO PM, which contains PEO in the outer shell of the micelles, may serve not only as a drug carrier in i.v. administration, but also has the advantages of decreasing the systemic concentration of free drug, inhibiting the intracellular drug uptake.

Bcl-x_L is a well characterized anti-apoptotic member of bcl-2 family, which is expressed in adult neurons, oligodendrocytes and T cells in CNS and plays an essential role in preventing neuronal cell death (7,47,48). Nesic-Taylor $et\ al.$, (7) reported that Bcl-x_L protein directed to injured spinal cord increased neuronal survival. This is consistent with the finding that administration of glucocorticoid after SCI increased Bcl-x_L expression. (48–51). Our RT-qPCR and Western blotting analyses also showed elevated Bcl-x_L mRNA and protein in spinal cord after delivery of MP/PM, compared to that detected in MP alone-delivery groups. The pharmacological profile of MP correlated well with the onset and duration of the pharmacological actions of MP on neurochemistry and neurophysiology in spinal cord tissues as other reported (1,2,38,42). Our results showed that the Bcl-x_L protein decreased by 16% at 7 h after SCI, consisting with 20% decreasing at the Bcl-x_L protein upon SCI reported by Nesic-Taylor $et\ al.$(7). They also indicated that direct injection of Bcl-x_L protein obtained 2 fold Bcl-x_L in spinal cord area and 60% of motoneurons could be preserved and protected after 24 h of SCI. We also found a significant increasing Bcl-x_L mRNA level (2.16 fold) at 7 h after delivery with MP/PM in SCI mouse, compared with that in SCI mouse. In conclusion, MP administered with PM instead of MP alone is likely to improve its bioavailability in both plasma and spinal cord. In addition, anti-apoptotic Bcl-x_L effect was significant upon MP/PM treatment in SCI model mouse.

ACKNOWLEDGEMENTS

REFERENCES

1. M. B. Bracken, M. J. Shepard, T. R. Holford, L., Leo-Summers, E. F. Aldrich, M. Fazl, M. Fehlings, D. L. Herr, P. W. Hitchon, L. F. Marshall, R. P. Nockels, V. Pascale, P. L. Perot, J. Piepmeier, V. K. Sonntag, F. Wagner, J. E. Wilberger, H. R. Winn, and W. Young. Administration of methylprednisolone for 24 or 48 hours or tirilazad mesylate for 48 hours in the treatment of acute spinal cord injury: results of the third national acute spinal cord injury randomized controlled trial. National acute spinal cord injury study. $JAMA$ **277**:1597–604 (1997).

2. J. L. Segal, B. F. Malthy, M. I. Langdorf, R. Jacobson, S. R. Brunnemann, and W. J. Jusko. Methylprednisolone disposition kinetics in patients with acute spinal cord injury. $Pharmacotherapy$ **18**:16–22 (1998).

3. J. Vaquero, M. Zurita, S. Oya, C. Aguayo, and C. Bonilla. Early administration of methylprednisolone decreases apoptotic cell death after spinal cord injury. $Histol.\ Histopathol.$ **21**:1091–102 (2006).

4. J. Xu, G. Fan, S. Chen, Y., Wu, X. M. Xu, and C. Y. Hsu. Methylprednisolone inhibition of TNF-alpha expression and NF-kB activation after spinal cord injury in rats. $Brain\ Res.\ Mol.\ Brain\ Res.$ **59**:135–142 (1998).

5. P. Yan, J. Xu, Q. Li, S., Chen, G. M. Kim, C. Y. Hsu, and X. M. Xu. Glucocorticoid receptor expression in the spinal cord after traumatic injury in adult rats. $J.\ Neurosci.$ **19**:9355–9363 (1999).

6. J. Qiu, O. Nesic, Z. Ye, H. Rea, K. N. Westlund, G. Y. Xu, D. McAdoo, C. E. Hulsebosch, and J. R. Perez-Polo. Bcl-$_{xL}$ expression after contusion to the rat spinal cord. $J.\ Neurotrauma.$ **18**:1267–1278 (2001).

7. O. Nesic-Taylor, D. Cittelly, Z. Ye, G. Y. Xu, G. Unabia, J. C. Lee, N. M Svrakic, X. H. Liu, R. J. Youle, T. G. Wood, D. McAdoo, K. N. Westlund, C. E. Husebosch, and J. R. Perez-Polo. Exogeneous bcl-xL fusion protein spares neurons after spinal cord injury. $J.\ Neursci.\ Res.$ **79**:628–637 (2005).

8. R. D. Stevens, A. Bhardwaj, J. R. Kirsch, and M. A. Mirski. Critical care and perioperative management in traumatic spinal cord injury. $J.\ Neurosurg.\ Anesthesiol.$ **15**:215–229 (2003).

9. C. Pozzi, P.G. Bolasco, G. B. Fogazzi, S. Andrulli, P. Altieri, C. Ponticelli, and F. Locatelli. Corticosteroids in IgA nephropathy: a randomised controlled trial. $Lancet$ **353**:883–887 (1999).

10. M. S. Nash. Known and plausible modulators of depressed immune functions following spinal cord injuries. $J.\ Spinal.\ Cord.\ Med.$ **23**:111–120 (2000).

11. H. Derendorf, H. Mollmann, M. Krieg, S., Tunn, C. Mollmann, J. Barth, and H. J. Rothig. Pharmacodynamics of methylpred-

nisolone phosphate after single intravenous administration to healthy volunteers. *Pharm. Res.* **8**:263–268 (1991).

12. J. C. Drummond, and S. S. Moore. The influence of dextrose administration on neurologic outcome after temporary spinal cord ischemia in the rabbit. *Anesthesiology* **70**:64–70 (1989).

13. L. C. Weaver, D. Gris, L. R. Saville, M. A. Oatway, Y. Chen, D. R. Marsh, E. F. Hamilton, and G. A. Dekaban. Methylprednisolone causes minimal improvement after spinal cord injury in rats, contrasting with benefits of an anti-integrin treatment. *J. Neurotrauma.* **22**:1375–1387 (2005).

14. K. L. Koszdin, D. D. Shen, and C. M. Bernards. Spinal cord bioavailability of methylprednisolone after intravenous and intrathecal administration: the role of P-Glycoprotein. *Anesthesiology* **92**:156–163 (2002).

15. C. M. Bernards, and T. Akers. Effect of postinjury intravenous or intrathecal methylprednisolone on spinal cord excitatory amino-acid release, nitric oxide generation, PGE(2) synthesis, and myeloperoxidase content in a pig model of acute spinal cord injury. *Spinal Cord* **44**:33–37 (2006).

16. A. Oka, M. Oda, H. Saitoh, A. Nakayama, M., Takada, and B. J. Aungst. Secretory transport of methylprednisolone possibly mediated by P-Glycoprotein in Caco-2 Cells. *Biol. Pharm. Bull.* **25**:393–396 (2002).

17. B. Davidson, and B. Roessler. Adenoviral-mediated gene transfer: Potential therapeutic applications. In M. G. Kaplitt, and A. D. Loewy (eds.), *Viral Vectors: Gene Therapy and Neuroscience Applications*, Academic, San Diego, 1997, pp. 173–189.

18. N. M. Boulis, N. E. Willmarth, D. K. Song, E. L., Feldman, and M. J. Imperiale. Intraneural colchicines inhibition of adenoviral and adeno-associated viral vector remote spinal cord gene delivery. *Neurosurgery* **52**:381–387 (2001).

19. G. S. Kwon, and K. Kataoka. Block copolymer micelles as long circulating drug vehicles. *Adv. Drug Deliv. Rev.* **21**:77–80 (1995).

20. A. V. Kabanov, P. Lemieux, S. Vinogradov, and V., Alakhov. Pluronic block copolymers: a novel functional molecules for gene therapy. *Adv. Drug Deliv. Rev.* **54**:223–233 (2002).

21. J. Liaw, T. Aoyagi, K. Kataoka, Y. Sakurai, and T. Okano. Permeation of PEO-PBLA-FITC polymeric micelles in aortic endothelial cell. *Pharm. Res.* **16**:213–220 (1999).

22. H. M. Aliabadi, D. R. Brocks, and A. Lavasanifar. Polymeric micelles for the solubilization and delivery of cyclosporine A: pharmacokinetics and biodistribution. *Biomaterials* **26**:7251–7259 (2005).

23. R. Gref, Y. Minamitake, M. T. Peracchia, V. Trubetskoy, V. Torchilin, and R. Langer. Biodegradable long circulating nanospheres. *Science* **263**:1600–1603 (1994).

24. M. Yokoyama, S. Fukushima, R. Uehara, K. Okamoto, K. Kataoka, Y. Sakurai, and T. Okano. Characterization of physical entrapment and chemical conjugation of adriamycin in polymeric micelles and their design for *in vivo* delivery to a solid tumor. *J. Control. Rel.* **50**:79–92 (1998).

25. J. Liaw, and T. C. Lin. Evaluation of PEO-PPO-PEO gels as a release vehicle for percutaneous fentanyl. *J. Control. Rel.* **68**:273–282 (2000).

26. E. V. Batrakova, S. Li, V. Alakhov, D. W. Miller, and A. V., Kabanov. Optimal structural requirements for pluronic block copolymers in modifying P-glycoprotein drug efflux transporter activity in bovine brain microvessel endothelial cells. *J. Pharmacol. Exp. Ther.* **304**:845–854 (2003).

27. S. M. Moghimi, C. Hunter, and J. C. Murray. Long-circulating and target-specific nanoparticles: theory to practice. *Pharmcol. Rev.* **53**:283–318 (2003).

28. D. C. Litzinger, A. M. Buiting, and N. Van Rooijen. Effect of liposome size on the circulation time and into organ distribution of amphipathic poly(ethylene glycol)-containing liposome. *Biochim. Biophys. Acta.* **1190**:99–107 (1994).

29. C. Allen, A. Eisenberg, J. Mrsic, and D. Maysinger. PCL-PEO micelles as a delivery vehicles for FK506: assessment of a functional recovery of crushed peripheral nerve. *Drug Deliv.* **7**:139–145 (2000).

30. D. M. Faulkner, S. T. Sutton, J. D. Hesford, B. C., Faulkner, D. A. Major, T. B. Hellewell, M. M. Laughon, G. T. Rodeheaver, and R. F. Edlich. A new stable pluronic F68 gel carrier for antibiotics in contaminated wound treatment. *J. Emerg. Med.* **15**:20–24 (1997).

31. Y. C. Chao, S. F. Chang, S. C. Lu, T. C. Hwang, W. H. Hsieh, and J. Liaw. Ethanol enhanced *in vivo* gene delivery with nonionic polymeric micelles inhalation. *J. Control. Rel.* **118**:105–117 (2007).

32. Y. C. Tong, S. F. Chang, C. Y. Liu, W. W. Y. Kao, C. H. Huang, and J. Liaw. Eye drop delivery of nano-polymeric micelle formulated genes with cornea-specific promoters. *J Gene Med.* **9**:956–966 (2007).

33. S. Y. Tsai, L. Y. Yang, C. H. Wu, S. F. Chang, C. Y. Hsu, C. P. Wei, S. J. Leu, J. Liaw, Y. H. Lee, and M. D. Tsai. Injury-induced Janus kinase/protein kinase C-dependent phosphorylation of growth-associated protein 43 and signal transducer and activator of transcription 3 for neurite growth in dorsal root ganglion. *J. Neurosci. Res.* **85**(2):321–331 (2007).

34. S. F. Chang, Y. Y. Sun, L. Y. Yang, S. Y. Hu, S. Y. Tsai, W. S. Lee, and Y. H. Lee. Bcl-2 gene family expression in the brain of rat offspring after gestational and lactational dioxin exposure. *Ann. N.Y. Acad. Sci.* **1042**:471–480 (2005).

35. Y. Hanazono, K. E. Brown, A. Handa, M. E. Metzger, D. Heim, G. J. Kurtzman, R. E. Donahue, and C. E. Dunbar. *In vivo* marking of rhesus monkey lymphocytes by adeno-associated viral vectors: direct comparison with retroviral vectors. *Blood* **94**:2263–2270 (1999).

36. C. Brand, E. Burkhardt, F. Schaeffel, J. W. Choi, and M. P. Feldkaemper. Regulation of Egr-1, VIP, and Shh mRNA and Egr-1 protein in the mouse retina by light and image quality. *Mol. Vis.* **28**:309–320 (2005).

37. S. F. Chang, H. Y. Chang, Y. C. Tong, S. H. Chen, F. C. Hsaio, S. C. Lu, and J. Liaw. Nonionic polymeric micelles for oral gene delivery *in vivo*. *Human Gene Ther.* **15**:481–493 (2004).

38. O. Majid, F. Akhlaghi, T. Lee, D. W. Holt, and A. Trull. Simultaneous determination of plasma prednisolone, prednisone, and cortisol levels by high-performance liquid chromatography. *Ther. Drug Monitor* **23**:163–168 (2001).

39. W. F. Ebling, S. J. Szefler, and W. J. Jusko. Methylprednisolone disposition in rabbits. Analysis, prodrug conversion, reversible metabolism, and comparison with man. *Drug Metab. Dispos.* **13**:296–304 (1985).

40. W. Piekosewski, F. S. Chow, and W. J. Jusko. Pharmacokinetic and pharmacodynamic effects of coadministration of methylprednisolone and tacrolimus in Rabbits. *J. Pharmacol. Exp. Ther.* **269**:103–109 (1994).

41. X. Zhang and R. Mehvar. Dextran-methylprednisolone succinate as a prodrug of methylprednisolone: dose-dependent pharmacokinetics in rats. *Int. J. Pharm.* **229**:173–182 (2001).

42. J. Schmidt, J. M. Metselaar, M. H. M. Wauben, K. V. Toyka, G. Strom, and R. Gold. Drug targeting by long-circulating liposomal glucocorticosteroids increases therapeutic efficacy in model of multiple sclerosis. *Brain* **126**:1895–1904 (2003).

43. J. S. Tan, D. E. Butterfield, C. L. Voycheck, K. D. Caldwell, and J. T. Li. Surface modification of nanoparticles by PEO/PPO block copolymers to minimize interactions with blood components and prolong blood circulation in rats. *Biomaterials* **14**:823–833 (1993).

44. J. M. Grindel, T. Jaworski, R. M. Emanuele, and P. Culbreth. Pharmacokinetics of a novel surface-active agent, purified poloxamer 188, in rat, rabbit, dog, and man. *Biopharm & Drug Disposit* **23**:87–103 (2002).

45. E. V. Batrakova, S. Li, Y. Li, V. Y. Alakhov, W. F. Elmquist, and A. V. Kabanov. Distribution kinetics of a micelle-forming block copolymer pluronic 85. *J. Control. Rel.* **100**:389–397 (2004).

46. V. P. Sant, D. Smith, and J. C. Leroux. Enhancement of oral bioavailability of poorly water-soluble drugs by PEO-PAAMA self assemblies. *J. Control. Rel.* **104**:289–300 (2005).

47. A. S. Parsadanian, Y. Cheng, C. R. Keller-Peck, D. M. Holtzman, and W. D. Snider. Bcl-xL is an antiapoptotic regulator for postnatal CNS neurons. *J. Neurosci.* **18**:1009–1019 (1998).

48. J. Schmit, R. Gold, L. Schnoroch, U. K. Zettl, H. P. Hartung, and K. V. Toyka. T-cell apoptosis *in situ* in experimental autoimmune encephalomyelitis following methylprednisolone pulse therapy. *Brain* **123**:1431–1441 (2000).

49. T. Y. Yune, S. J. Kim, S. M. Lee, Y. K. Lee, Y. J. Oh, Y. C. Kim, G. J. Markelonis, and T. H. Oh. Systemic administration of 17 beta-estradiol reduces apoptotic cell death and improves func-tional recovery following traumatic spinal cord injury in rats. *J. Neurotrauma.* **21**:293–306 (2004).

50. G. Cao, W. Pei, H. Ge, Q. Liang, Y. Luo, F. R. Sharp, A. Lu, R. Ran, S. H. Graham, and J. Chen. *In vivo* delivery of a bcl-xl fusion protein containing the TAT protein transduction domain protects against ischemic brain injury and neuronal apoptosis. *J. Neurosci.* **22**:5423–5431 (2002).

51. S. Y. Tsai, P. Y. Chiu, C. P. Yang, and Y. H. Lee. Synergistic effects of corticosterone and kainic acid on neurite outgrowth in axotomized doral root ganglion. *Neurosci.* **114**:55–67 (2002).